Edinburgh, Scotland
EURONOISE 2009
October 26-28

Automatic liner optimisation for bypass ducts

Jeremy Astley, Iansteel Achunche, Rie Sugimoto
ISVR, University of Southampton, Southampton, SO17 1BJ, United Kingdom

ABSTRACT

Acoustic liners are placed in the intake and bypass ducts of turbofan aeroengines to reduce the environmental impact of turbomachinery noise at take-off and approach. The fan stage is the principal source of turbomachinery noise for a modern High Bypass Ratio turbofan engine. The most common construction for a turbofan liner is a curved panel formed from a layer of honeycomb material which is separated from the flow by a porous facing sheet, and fixed to a rigid backing sheet. The acoustic performance of such panels depends upon the source spectrum, the honeycomb depth and the facing sheet resistance. The study reported here explores potential new approaches to the optimisation of multiple-segment, acoustic liners in the bypass duct to reduce environmental noise. A finite element code, Actran-TM, is used to predict the acoustic transmission loss through a bypass duct and a sequence of such computations is integrated within an automated optimisation code SOFT to select optimal liner parameters (liner depth and facing sheet resistance). The optimisation procedure is based on minimising the A-weighted transmitted acoustic power. The method is demonstrated for an idealised annular duct but the objective of the current study is to determine whether it is feasible for application to real turbofan ducts.

1. INTRODUCTION

The basic mechanism of sound absorption by turbofan duct liners is the conversion of acoustic energy to heat by viscous dissipation. An oscillating pressure field due to an acoustic disturbance incident on an acoustically lined portion of the duct wall drives air through apertures in a porous facing sheet. Acoustic energy is either dissipated directly by viscous forces in the aperture or converted into vortical kinetic energy. The device is locally reacting since the pressure field in each cell is independent of that in its neighbours. The basic absorption mechanism for a pressure disturbance propagating along the surface is illustrated in Figure 1.

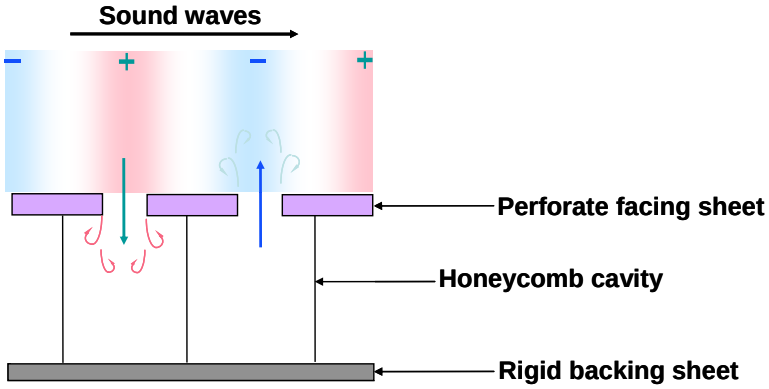

Figure 1: Single cavity liner model showing, movement of sound waves in and out of perforate holes.

The acoustic performance of the liner is characterized by the specific acoustic impedance, $Z(\omega)$, defined as the ratio $p : u_n$ where p and u_n are the complex pressure amplitude at the surface, and the complex mean velocity amplitude normal to the surface, for pressure fluctuations at a given frequency ω. For a single cavity liner as shown in Figure 1

$$Z(\omega) = R + i\rho c(kl - \cot(kd)) \tag{1}$$

where R is the (dimensional) resistance of the facing sheet, k (=ω /c) is the acoustic wave number, l is the mass inertance of the facing sheet, d is the cavity depth, ρ is the density and c is the stagnation sound speed. The acoustic performance of the liner depends upon frequency (through the parameter k) and can be 'tuned' to absorb acoustic energy from specific regions of the source spectrum by judicious choice of the cell depth and the facing sheet resistance.

Calculating the reduction in noise radiated by the nacelle for a specific liner configuration is a non-trivial exercise. This is the necessary 'forward problem' which must be solved in a liner optimisation. In this article we focus on an idealized, uniform, annular, bypass duct. A finite element shell program B-induct[1] which calls the commercial aeroacoustic code Actran-TM is used to predict the acoustic transmission loss in the duct. The liner has the construction shown in Figure 1. The computation of the acoustic field in the duct for a given liner is performed in the presence of mean flow. A multimodal source is assumed which consists of specific tones which protrude from a multimode spectrum in which all propagating modes are present with equal acoustic power. B-induct is embedded within an in-house Roll-Royce optimisation suite, SOFT[2]. This is used to select the resistance and depth of the several liner segment(s) which maximise the transmission loss over a range of frequencies. Results are obtained for single and multiple liners.

The simplest case (Figure 2a) is a uniform annular segment with the same liner on the inner and outer walls. The liner impedance is defined by two variables (depth and resistance). The procedure can be validated by comparing the 'optimising' values of resistance and depth to values obtained from two-dimensional contour plots of transmission loss as a function of resistance and depth.

When multiple liner segments are present - for example when two axial segments of impedance Z_1 ad Z_2 are present as shown in figure 2b - more that two design variables are involved and the optimized values cannot be validated against two-dimensional contour plots. The reasonableness of the optimized solution can however be checked by noting that the transmission loss should at least exceed that of the optimal single liner case.

Results are presented first for the case where a single liner segment is optimised at a single frequency and then for the case where two axial segments are optimized, again at a single frequency. Finally, a lined segment is optimised over a range of frequencies by using a cost function which uses an A-weighted power spectrum at 1/3-octave centre frequencies from 500 Hz to 10 kHz.

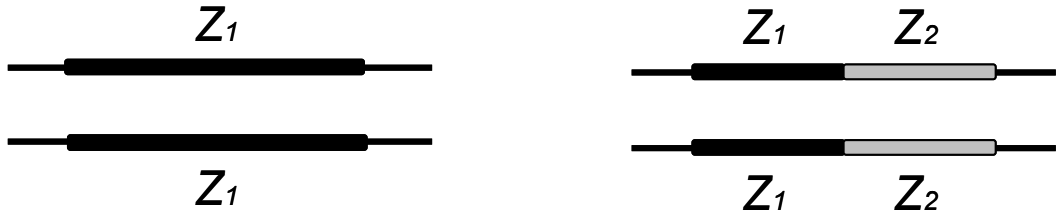

(a) (b)

Figure 2: Sketch of inner and outer wall of a uniform bypass duct showing different arrangements of liner impedances Z_1 and Z_2.

2. CALCULATING THE TRANSMISSION LOSS: B-INDUCT

B-induct is a shell program which performs ACTRAN-TM[3] analysis of the in-duct domain of an axisymmetric bypass duct. The computational domain extends from the input plane behind the outlet guide vanes (OGVs) to the bypass exhaust; a region in which the sound field is scattered by the duct geometry and absorbed by the acoustic liners (see Figure 3). B-induct creates an ACTRAN-TM mesh for this region which takes into account the frequency and mean flow Mach number. A regular mesh generated by B-induct for a uniform annular duct is shown in Figure 4.

Modal boundary conditions are then imposed at the input and exhaust planes, expressed in terms of hard-walled annular modes. At the input plane, the acoustic power of each incident mode is prescribed. Reflected mode amplitudes are computed during the analysis by assuming an anechoic termination for noise propagating upstream. At the exhaust plane, reflections from the nozzle are neglected and the sound field is assumed to consist only of downstream propagating modes. B-induct duct then computes the mean flow solution using an in-built compressible FE Euler solver, interpolates the mean flow velocities onto the FE acoustic mesh and executes a sequence of Actran-TM acoustic analyses for a prescribed set of frequencies and azimuthal orders. These are executed within the B-induct shell and the reflected and transmitted acoustic power for each set of incident modes is extracted from the output data. If P_I and P_T denote the incident power (at the input plane) and the transmitted power (at the exhaust plane) the transmission loss ΔPWL in decibels (dB) is given by,

$$\Delta PWL = 10\log_{10}\left(\frac{P_I}{P_T}\right) \quad . \tag{2}$$

In cases where the optimisation is performed over a range of frequencies, a weighted average of the values of transmission loss at each frequency is used, with weighting factors taken from the standard 'A-weighting' curve.

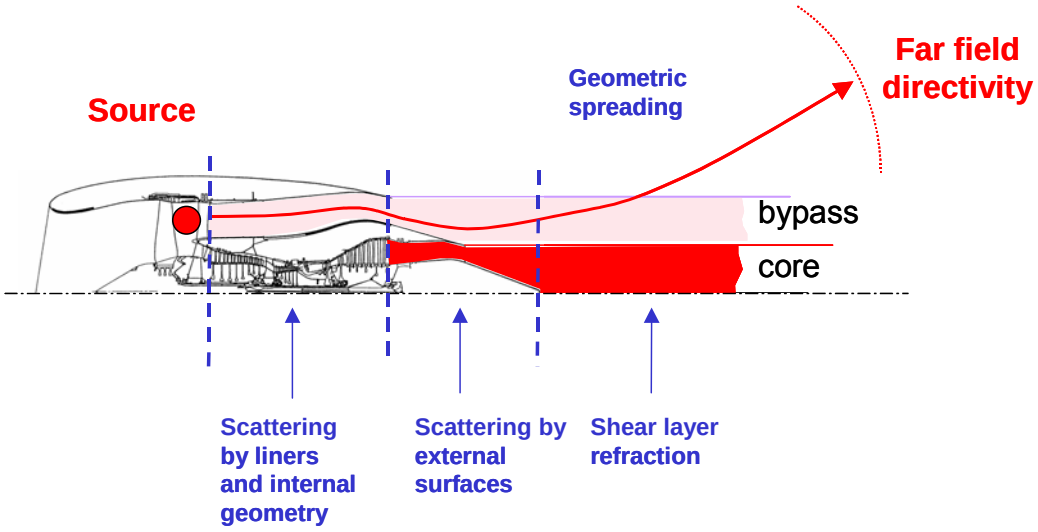

Figure 3: The acoustic transmission path from the fan stage of a HBR turbofan engine to the far field

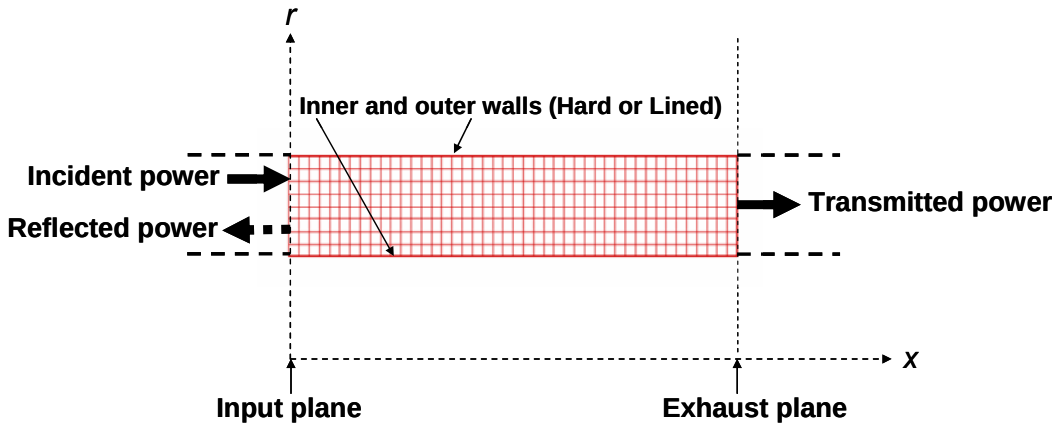

Figure 4: Uniform bypass duct showing FE mesh generated by B-induct.

3. OPTIMISATION STRATEGY: SOFT

The optimisation of ΔPWL is performed by using global and local search algorithms within the Rolls-Royce in-house, optimisation suite, SOFT[2]. SOFT provides a link between simulation code(s) and a library of optimisation algorithms. In the current study, the simulation code is B-induct. Starting from an initial guess for liner resistance and depth, B-induct is executed within SOFT to obtain the transmission loss for a sequence of liner specifications. The liner resistances and depths for successive evaluations can either be chosen deterministically or stochastically depending upon the algorithm which is used. Figure 5 illustrates the general sequence which is followed within the SOFT optimisation suite.

A choice of optimisation algorithm(s) is available within the optimisation set-up and must be selected by the user. The user also specifies the design range (bound constraints) for each of the design variables. In all of the calculations presented here, the non-dimensional resistance *r* of each liner varies between 0 and 5. The liner depth is allowed to vary between *0* and π/k when optimizing at a single frequency (k is the wave number ω/c). The single cavity liner model which is used in this study, gives a non-dimensional reactance, $\chi' = kl - \cot(kd)$ which repeats for *kd* > π. The smallest liner depth is usually the most desirable, and the depth range is therefore constrained to exclude higher values. In cases where the transmission loss is calculated over a range of frequencies, the upper bound of the liner depth is set to *50mm (~2inches)* which is a reasonable upper bound for current liner installations.

The numerical values of the dimensional resistance (in *kg/m^{2}s)* and depth (in *mm)* are however disparate within these ranges. Since the optimisation algorithms perform most effectively when the design space is isotropic and the design variables are of order 1, the liner parameters are normalised prior to optimisation to define a design space in which all the variables vary between 0 and 1. A hybrid search is then used. From the SOFT library a global genetic algorithm (Adaptive Range Multi-Objective Genetic Algorithm, "ARMOGA"[4]) is chosen, followed by a Dynamic Hill Climbing[6] (DHC) search. The global search ensures that the whole design space is explored so as to avoid local optima, and the local search refines the global optimum to obtain a more precise solution.

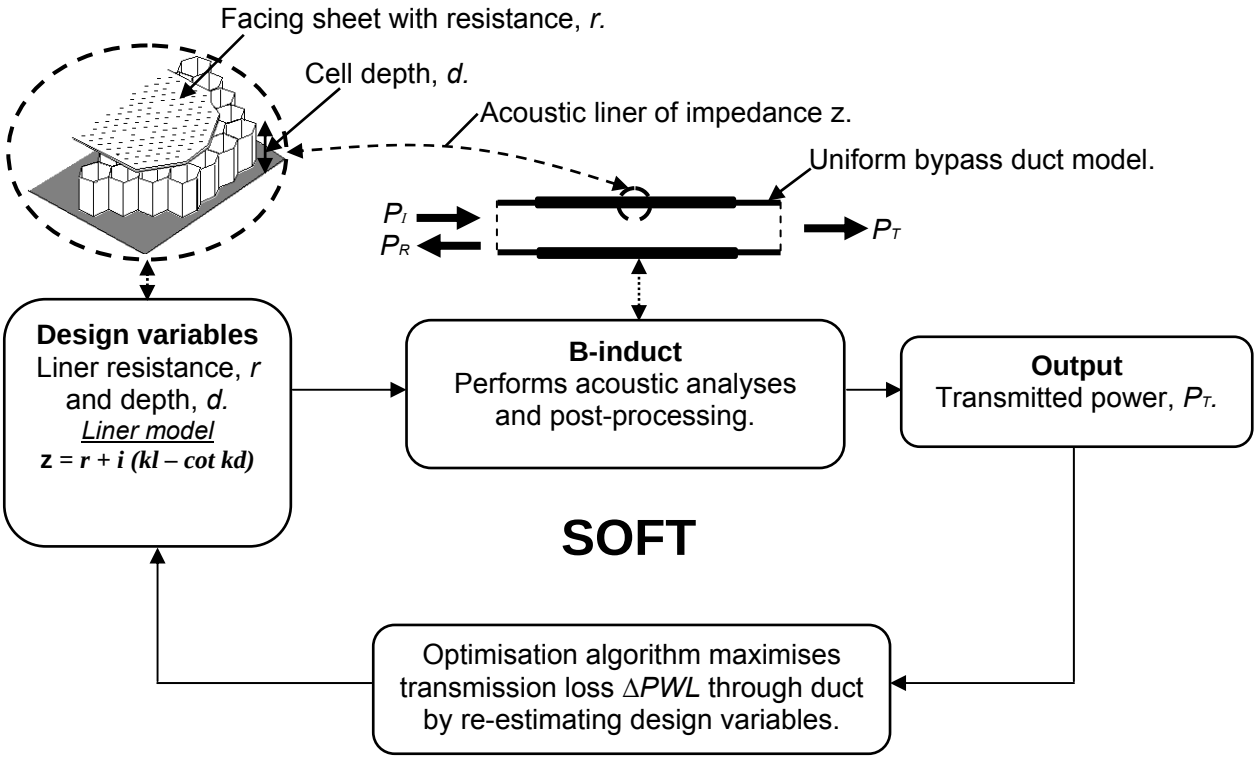

Figure 5: Liner impedance optimisation process, using B-induct within SOFT.

A. The 'ARMOGA' global search

ARMOGA[4] is a genetic algorithm[5] which has the ability to change the search region based on the best designs obtained from previous generations. This facility stems from the `adaptive range' capability of the algorithm and technically requires more than one cost function (multi-objective) to be considered in the optimisation process[4]. This is because the range adaptation process makes use of a set of optimal solutions (a Pareto set) obtained from assigning different weights to a combination of cost functions. For a single objective optimisation as presented in this paper, an ARMOGA search reduces to a simple GA search.

GAs use the ideas of natural selection and genetics to iteratively transform a set of designs called a 'population' into a new population of 'off-spring' designs (see Figure 6) through a crossover[5] process. The performance of the 'ARMOGA' GA in SOFT is determined by the population size and by the number of generations. The population size represents the number of randomly chosen designs and the number of generations is the number of times the initial population is transformed.

B. The local Dynamic Hill climbing (DHC) search

The DHC algorithm in SOFT comprises an inner loop and an outer loop. The inner loop consists of an efficient hill climbing technique for locating local optima and the outer loop searches random regions of the design space so that it is well explored. In the current application, since the DHC search has been preceded by a global GA search, the random re-start capability (outer loop) of the DHC algorithm is not required, and only the inner loop is used.

For an *n*-dimensional problem, the inner loop maintains a list of 2*n* vectors, *n* of which form an orthogonal basis set for the search space. The other *n* are the negations of these vectors. Also included are two additional vectors called gradient vectors that are functions of the last two directions the algorithm has moved in.

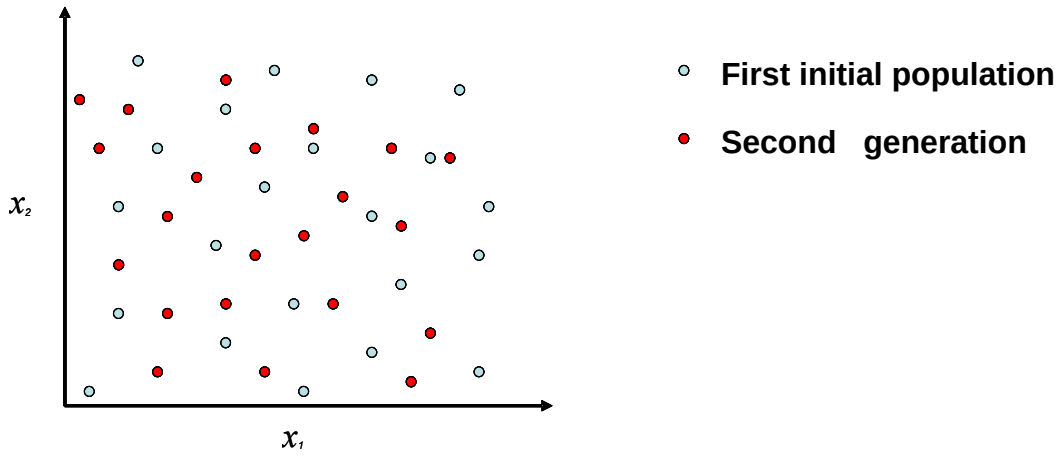

Figure 6: Illustration of initial and off-spring designs in GA search for problem with design variables x_1 and x_2 (22 designs in initial population).

The operation of the DHC method is illustrated in Figure 7. In the general case of an *n*-dimensional problem, the inner loop maintains a list of 2*n* vectors, *n* of which form an orthogonal basis set for the search space and the other *n* are the negations of these vectors. Also included are two additional vectors called gradient vectors that are functions of the last two directions that the algorithm has moved in. Starting from an initial point $\underline{\mathbf{x}}$, and with the vector $\underline{\mathbf{v}}_i$ that has the largest magnitude, DHC evaluates the point $\underline{\mathbf{x}}+\underline{\mathbf{v}}_i$ and compares it to the value of the function f at $\underline{\mathbf{x}}$. If the aim is to minimise the cost function, and if $f(\underline{\mathbf{x}}+\underline{\mathbf{v}}_i) < f(\underline{\mathbf{x}})$, then $\underline{\mathbf{x}}+\underline{\mathbf{v}}_i$ becomes the new 'best' point, and the process is repeated. However, if $f(\underline{\mathbf{x}}+\underline{\mathbf{v}}_i) > f(\underline{\mathbf{x}})$ the magnitude of $\underline{\mathbf{v}}_i$ is halved and the vector with the next largest magnitude is used. The algorithm continues to update the magnitudes of the vectors and the current point until if finds a point from which the function cannot be further decreased , as defined by a minimum length of the vector $\underline{\mathbf{v}}$ set by the user. Figure 7 shows a two-dimensional search space with orthogonal vectors and a gradient vector required to track the curvature of the search space.

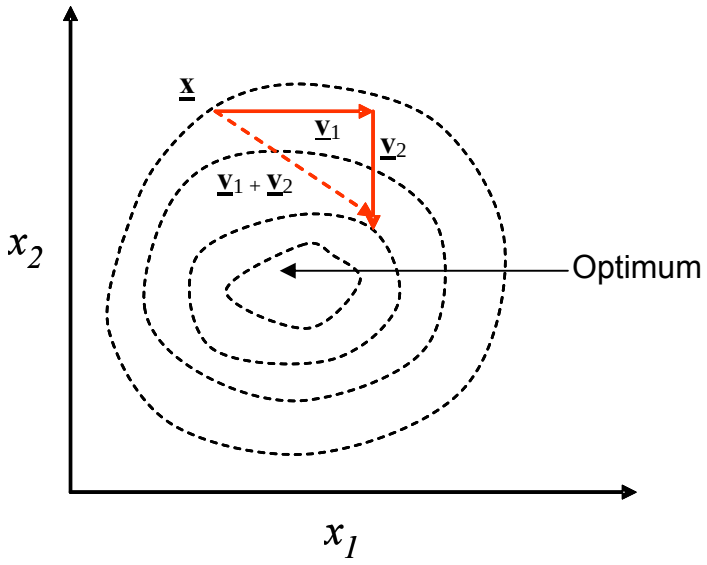

Figure 7: Search space (for design variables x_1 and x_2) showing orthogonal vectors $\underline{\mathbf{v}}_1$ and $\underline{\mathbf{v}}_2$, and gradient vector $\underline{\mathbf{v}}_1 + \underline{\mathbf{v}}_2$

5. RESULTS

A. Single impedance, single frequency optimisation

The results obtained by optimising a uniform liner for an annular duct of the dimensions shown in Figure 8, at frequencies of *1.0* and *2.0* kHz are shown in Figure 9 and Table 1. The contours shown in Figure 9 are obtained by evaluating the transmission loss on a regular grid spanning the design space. The red dots are the ARMOGA points and the blue lines track the progress of the DHC search. For both frequencies the SOFT optimisation correctly locates the maximum value of the transmission loss, as indicated by the contour plot.

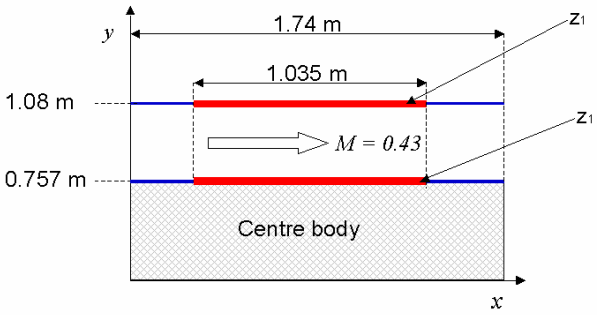

Figure 8: Uniform bypass duct with single impedance z_1.

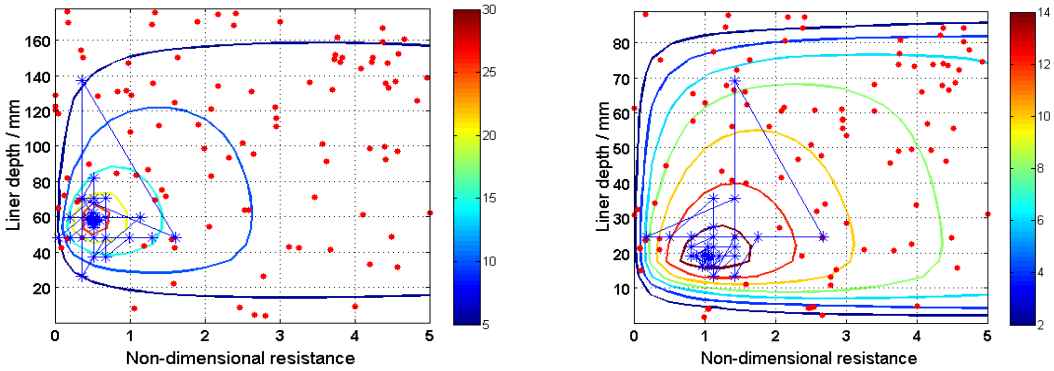

(a) 1000 Hz (b) 2000 Hz

Figure 9: Superposition of SOFT hybrid search on a two-dimensional contour plot of transmission loss ΔPWL, as a function of resistance and depth. The red dots show the evaluation points from the ARMOGA (global) search and the blue crosses show the path of the DHC (local) search.

Table 1: Optimised resistances and liner depths for each frequency.

Freq / Hz (modes)	1000 (79)	2000 (279)
r_1 d_1 / mm	*0.520* *58.6*	*1.044* *19.1*
ΔPWL / dB	*36.06*	*15.53*
CPU time	*14m* *151 eval.*	*1h 13m* *151 eval.*

B. Double impedance, single frequency optimisation

The results obtained from an optimization of a two segment liner with impedances z_1 and z_2 (see Figure 10) are shown in Table 2. The liners are optimised for frequencies of *1.0* and *2.0* kHz. Since four liner parameters are now involved in the optimisation, the result cannot be checked against simple 2D contours. However, the procedure is partially validated by noting that for both frequencies the optimum values of transmission loss are somewhat larger than for the single liner case, as must be the case given that the latter is a subset of the former.

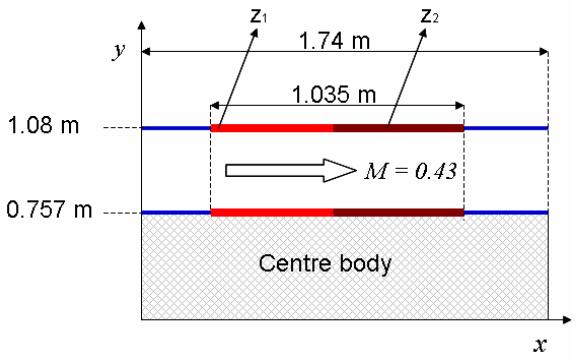

Figure 10: Uniform bypass duct with double impedance segments z_1 and z_2.

Table 2: Optimised resistances and liner depths for each frequency.

Freq / Hz (modes)	1000 (79)	2000 (279)
r_1 d_1 / mm r_2 d_2 / mm	0.569 60.0 0.473 57.9	1.26 21.2 0.717 17.4
ΔPWL / dB	36.49	16.34
CPU time	32m 23s 326 eval.	2h 13m 39s 278 eval.

C. Single impedance, multiple frequency optimisation (500 Hz to 10 kHz)

In the multiple frequency optimisation, the transmission loss ΔPWL is calculated for an A-weighted source spectrum at 1/3-octave centre frequencies from 500 Hz to 10 kHz. Figure 11 shows an A-weighted power spectrum for the case of a uniform acoustic power across all frequencies

Figure 11: A-weighted power spectrum for the case of uniform acoustic power at all frequencies

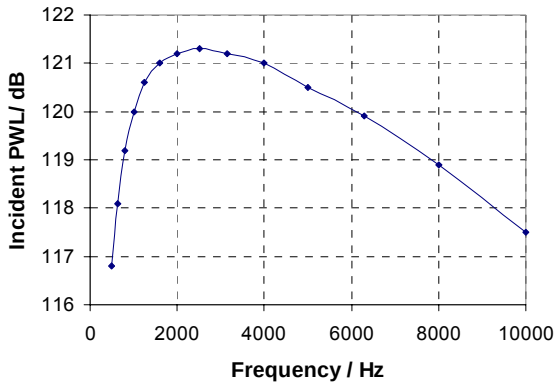

The results of the optimisation are shown in Figure 12 and Table 3. In Figure 12 the ARMOGA and DHC evaluations of the transmission loss are shown on a two-dimensional contour plot against *r* and *d* obtained by computing the transmission loss independently at a regular grid of points. The SOFT optimisation clearly captures the global optimum.

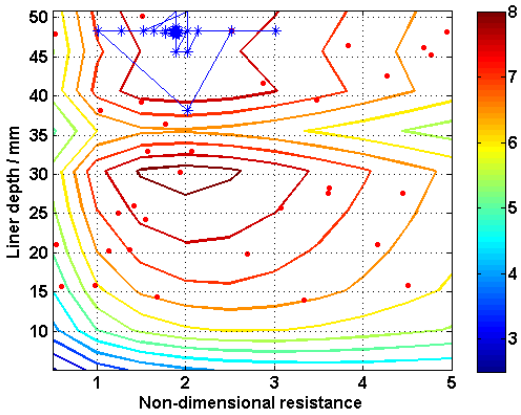

Figure 12: Superposition of SOFT hybrid search on a two-dimensional contour plot of transmission loss ΔPWL, as a function of resistance and depth. The red dots show the evaluation points from the ARMOGA (global) search and the blue crosses show the path of the DHC (local) search.

Table 3: Optimised impedance and liner depth.

Freq / Hz	**500 to 10 kHz**
r	***1.89***
d / mm	***48.1***
ΔPWL / dB	***8.57***
CPU time	***131 hr 29m 54s***
	77 eval.

6. CONCLUSION

In this paper, a finite element propagation code has been integrated within the Rolls-Royce optimisation suite SOFT and used to calculate optimum liners for single and multiple frequencies. An idealised (uniform) bypass was considered. The results have been fully and partially validated for single and double liner segments respectively.

Figures for CPU time are included in Tables 1-3. These relate to computations on a single processor and do not exploit more advanced solvers which are now available within ACTRAN-TM. Based on speed-up for other computations performed by the authors using more recent versions of this code, it is likely that the times given here can be reduced by an order of magnitude with little additional effort. This would bring the CPU time for the final A-weighted optimisation to less than one day well within acceptable values for industry application in this type of approach. It is also worth observing that while the current computations have been executed on a uniform annular duct, no additional computational effort is involved in applying this procedure to realistic axisymmetric, bypass-duct geometries. Full validation of the results for realistic multi-segment liners will however be more challenging since no obvious benchmark cases exist.

ACKNOWLEDGEMENTS

The work reported here was supported by Rolls-Royce plc within a more extensive programme of research on aircraft noise undertaken at the Rolls-Royce University Technology Centre in Gas Turbine Noise based at the Institute of Sound and Vibration Research. The second author is supported jointly by Rolls-Royce plc and the Engineering and Physical Sciences Research Council (EPSRC), within the Engineering Doctorate programme in transport engineering at the University of Southampton. The authors are indebted to Shahrokh Shahpar at Rolls-Royce for his advice on the use of SOFT.

REFERENCES

1. R. Sugimoto, B-induct users' manual, shell program for ACTRAN in-duct analysis for bypass ducts. ISVR, University of Southampton, UK, November 2004.

2. S. Shahpar, SOFT, "A new design and optimisation tool for turbomachinery", In Evolutionary methods for design, optimisation and control *2002, Giannakoglou, K. and Tsahalis, D. and Periaux, J. and Papailiou, K. and Fogarty, T*.

3. Actran – TM 2006 users' manual. Free Field Technologies, Louvain–La–Neuve, Belgium, 2006.

4. D. Sasaki and S. Obayashi, Efficient search for trade-offs by adaptive range multi-objective genetic algorithms. JOURNAL OF AEROSPACE COMPUTING, INFORMATION AND COMMUNICATION, 2: 44 – 64, 2005.

5. D.E. Goldberg. Genetic Algorithms in Search, Optimization and Machine Learning. Addison-Wesley, 1989.

6. D. Yuret and M. de la Maza. Dynamic hill climbing: overcoming the limitations of optimization techniques. *In the second Turkish symposium on artificial intelligence and neural networks*, pages 254 – 260, 1993.